Dynamical Behavior of the Quantum Periodically Kicked Harmonic Oscillator

1993 Commun. Theor. Phys. 19 289

(http://iopscience.iop.org/0253-6102/19/3/289)

Commun. Theor. Phys. 19(1993)289–294

Vol. 19, No. 3

Dynamical Behavior of the Quantum Periodically Kicked Harmonic Oscillator

Zong-Fu JIANG
Institute of Physics, Chinese Academy of Science, P.O. Box 603, Beijing 100080, China
(Received June 30, 1992; Revised August 21, 1992)

Abstract

We explore the properties of the quantum kicked harmonic oscillation governed by the Hamiltonian $H = \frac{1}{2}p^2 + \frac{1}{2}\omega_0^2 x^2 - K\cos x \sum_{n=-\infty}^{\infty}\delta(t/T - n)$. *The classical version of this model is known to exhibit certain type of stochastic behavior. We reduce the quantum equation of the model to quantum mapping equations. Numerical results of the mappings show that the behavior of the average energy as a function of time depends on the ration of the frequency of the external* $(2\pi/T)$ *and that of the unperturbed system* ω_0. *The energy increases first very rapidly and then the energy growth saturates for irrational* $\omega_0 T/2\pi$. *The break time is independent of the strength of the external force, but is roughly proportional to* $1/\omega_0 T$. *For a fixed rational* $\omega_0 T/2\pi$, *the energy is damped oscillation for smaller* T, *and it is seemingly recurrent with time in the sense of Hogg and Huberman. In both cases, these behaviors of energy are independent of the strength of the external force and differ from the behavior of the quantum kicked rotator.*

I. Introduction

Since the work of Casati *et al.*[1], many works have been devoted to understanding the time-dependent quantum systems beyond perturbation expansions. One of their motivations was to study whether the complex dynamics of general classical nonintegrable systems has any counterpart in quantum systems. The most popular model for this study is the rigid rotator submitted to periodic kicks. The classical counterpart of this model, described by the so-called " standard mapping"[2], is a well-known example of chaotic behavior. The energy of the classical kicked rotator grows with time in a chaotic way following the diffusion law $\langle E\rangle \sim t$ provided the perturbation is sufficiently large. In the quantum case several important discoveries have been made. When the external frequency and natural quantum frequency have simple rational ratios, the numerical results show that the average energy of the system increases quadratically in time[1,3]. By analogy with Anderson localization, Grempel *et al.* suggested that the irrational cases should lead to states localized in p space and hence must have bound energy[4]. Although the results of the simplest system have been applied in the studies of the quantum chaos of some complex systems, such as a hydrogen atom in a strong magnetic field, a rich variety of new physical phenomena[5] requires more detailed theoretical study with more adequate model. We here choose the kicked harmonic oscillator (KHO) as an example to explore the dynamical properties of a more complex system whose classical counterpart exhibits certain type of stochastic behavior.

The KHO problem is equivalent to the problem of the motion of a particle in a constant magnetic field and in the field of an electrostatic wave packet. The equation of particle motion in an external uniform magnetic field B_0 and an electrostatic wave that propagates orthogonally to the magnetic field (along the x-axis) is

$$\ddot{x} + \omega_0^2 x = \frac{\epsilon\omega_0}{k}\sin(kx - \Omega t), \tag{1}$$

where $\omega_0 = eB_0/mc$ is the cyclotron frequency. A more general case is that the disturbed wave packet contains a great number of plane waves

$$\ddot{x} + \omega_0^2 x = \frac{e}{m}\sum_k E_k \sin(kx - \omega_k t). \tag{2}$$

Choosing a certain special form of the wave packet $E_k = \text{const.} = E_0$, $k = \text{const.} = k_0$ and $\omega_k = n\Delta\omega\,(n = 0, 1, \cdots)$ and for a very large number of modes, equation (2) reduces to[6]

$$\ddot{x} + \omega_0^2 x = \frac{eE_0}{m}\sin(k_0 x)\sum_{m=-\infty}^{\infty}\delta\Big(\frac{t}{T} - n\Big) \tag{3}$$

with $T = 2\pi/\Delta\omega$, where $\Delta\omega$ is the frequency separation of the neighboring mode in the wave packet. Replacing disturbance amplitude $eE_0/m\sin(k_0 x)$ by a general function $f(x)$, equation (3) also represents the motion of collision between two binding pluse beams moving in opposite directions in the high energy cyclotron[7]. The following results might be useful for the discussion of the irregular collisions.

The classical chaotic motion of Eq. (3) has been widely studied[5–9]. We here are mainly to explore the quantum behavior of Eq. (3). In Sec. II, we derive and discuss the quantum mapping equations, and present our numerical results for the quantum problem. Brief concluding remarks are given in Sec. III.

II. Quantum Analysis of the KHO

2.1 Model

The Hamiltonian of Eq. (3) is given by[6]

$$H = \frac{1}{2}p^2 + \frac{1}{2}\omega_0^2 x^2 - K\cos x\sum_{n=-\infty}^{\infty}\delta\Big(\frac{t}{T} - n\Big), \tag{4}$$

where x is the displacement, p is the momentum and ω_0 is the frequency of harmonic oscillator, K is the maximun amplitude of kick, and we here have chosen the oscillator mass unit $m = 1$ and $k_0 = 1$. The quantum analogy of the Hamiltonian (4) is obtained by substituting $p \to -i\hbar\frac{\partial}{\partial x}$, so that the Schrödinger equation for wave function $\phi(x, t)$ becomes

$$i\hbar\frac{\partial\phi}{\partial t} = \Big[-\frac{1}{2}\hbar\frac{\partial^2}{\partial x^2} + \frac{1}{2}\omega_0^2 x^2 - K\cos x S(t)\Big]\phi, \tag{5}$$

where $S(t) = \sum_{n=-\infty}^{\infty}\delta(t/T - n)$. Since equation (5) becomes a model of free harmonic oscillator at $K = 0$, it is convenient to expand the wave function $\phi(x, t)$ in terms of the free harmonic oscillator eigen functions $\phi_n = \langle x|n\rangle$

$$\phi(x, t) = \sum_{n=-\infty}^{\infty} a_n(t)\phi_n. \tag{6}$$

The Schrödinger equation is again solved by considering the effect of the kick separately. Introducing

$$v_{nm} = \frac{\langle n|v(x)|m\rangle}{\exp(\hbar/2\beta^2)} \tag{7}$$

we obtain

$$\frac{\partial a_n}{\partial t} = -iE_n a_n - ikS(t)\sum_{n=-\infty}^{\infty} v_{nm}a_m. \tag{8}$$

Here $v(x) = \cos x$, $\beta = \sqrt{\hbar/2\omega_0}$ and $E_n = \epsilon_n/\hbar$, where $\epsilon_n = (n+1/2)\hbar\omega_0$ is the free oscillator energy eigenvalues, and k is

$$k = \frac{KT}{\hbar}\exp\Big(\frac{\beta^2}{2}\Big). \tag{9}$$

By writting further

$$a_n = \exp(-iE_n t)b_n\,, \tag{10}$$

we have

$$\frac{\partial b_n}{\partial t} = -ikS(t)\sum_{m=-\infty}^{\infty} w_{nm}b_n \tag{11}$$

with

$$w_{nm} = v_{nm}\exp[i(E_n - E_m)t]\,. \tag{12}$$

Between kicks $S(t) = 0$, one has simply $\partial b_n/\partial t = 0$ so that

$$b_n^-(N) = b_n^+(N-1)\,, \tag{13}$$

where N denotes the kick and $+(-)$ denotes the moment just after (before) the kick. During the infinitesimal interval of a kick, equation (8) can be integrated

$$b_n^+(N) - b_n^-(N) = -\frac{ik}{2}\Big\{\sum_{m=0}^{\infty} w_{nm}(N)[b_m^+(N) + b_m^-(N)]\Big\}\,. \tag{14}$$

Finally using Eq. (12), we obtain the quantum mapping

$$b_n^+(N) + i\frac{k}{2}\sum_m w_{nm}(N)b_m^+(N) = b_n^+(N-1) - i\frac{k}{2}\sum_m w_{nm}(N)b_m^+(N-1)\,. \tag{15}$$

Dropping the superscript $+$ and with obvious matrix notations, the mapping (15) can be written as

$$b(N) = \frac{I - i(k/2)w(N)}{I + i(k/2)w(N)}b(N-1)\,, \tag{16}$$

where $w_{nm}(N) = v_{nm}\exp[i(n-m)\alpha N]$, giving $b(N)$ at time (N) in terms of $b(N-1)$ at time $(N-1)$. The form of Eq. (15) is similar to the mapping for kicked quantum rotator[3], but very different in detail. Using Eqs. (6) and (15), we could obtain $\phi(x, N)$ in terms of $\phi(x, N-1)$. But in the calculations of interest here, the $b(N)$ energy-representation is more useful. Before turning to these calculations, let us discuss w_{nm} and the mapping of Eq. (15).

It is convenient to introduce the raising and lowering operators S^+ and S^-:

$$S^{\pm} = \beta'(p \pm i\omega_0 x)\,, \tag{17}$$

where $\beta' = \beta/\hbar$, and we have

$$[S^-, S^+] = 1\,, \qquad S^-|n\rangle = \sqrt{n}\,|n-1\rangle\,, \qquad S^+|n\rangle = \sqrt{n+1}\,|n+1\rangle \tag{18}$$

and

$$x = i\beta(S^- - S^+)\,, \qquad p = i\beta(S^- + S^-)\,. \tag{19}$$

Thus one has

$$\cos x = \frac{1}{2}(e^{ix} + e^{-ix}) = \frac{1}{2}e^{\beta^2/2}[e^{-\beta s^-}e^{\beta s^-} + e^{\beta s^-}\cdot e^{-\beta s^+}]\,. \tag{20}$$

We here have used Eq. (18) and $e^{\hat{A}}e^{\hat{B}} = e^{\hat{A}+\hat{B}+[\hat{A},\hat{B}]/2}$. Expanding Eq. (20) in a power series in S^+ and S^-, and using Eq. (18), we find

$$v_{nm} = \frac{1}{2}\sum_{l\geq 0, l\geq m-n}^{\infty} C_{nm,l}\,, \tag{21}$$

where

$$C_{nm,l} = [(-1)^l + (-1)^{n+l-m}]\frac{\beta^{n-m+2l}(n+l)!}{l!(n+l-m)!\sqrt{m!n!}}\,. \tag{22}$$

Finally from Eq. (12), we obtain

$$w_{nm} = \frac{1}{2} e^{i(n-m)N\omega_0 T} \sum_{l\geq 0, l\geq m-n}^{\infty} C_{nm,l}\left(\frac{\hbar}{\omega_0}\right). \tag{23}$$

Simply calculating Eq. (21) shows that 1) $C_{nm,l}$ rapidly approach zero as increasing l, that means even the sum on l is infinite, the $C_{nm,l}$ coefficients become negligible outside certain range; 2) when $|m-n| \geq 10$, $C_{nm,l} \sim 0$, thus we have $w_{nm} \sim 0$, that means most of the off-diagonal matrix elements of $w(N)$ are zero. Thus for reasonable size k-values starting from only one (or a few initially nonzero $b_n(0)$), we may iterate through many periods T before the increasing number of nonzero $b_n(N)$ exceeds the practical limitations of a large computer. Next, let us observe that the classical mapping depends on the parameters K and α. While the quantum mapping depends separately and complexly on K, ω and T. From Eqs. (9) and (23), one also notes that the KHO will be very different from the kicked rotator. In the kicked rotator, the quantum motion differs greatly from its classical motion in the case of small k and large τ for fixed $K = k\tau$[1]. In KHO, although equation (23) is invariant to replacement of α by $\alpha + 2\pi$, one can increase or decrease k in order to keep K fixed by changing T and ω_0 in different ways. That means various k might affect the result of the motion of the quantum mapping. In the following, we will give numerical results of KHO.

2.2 Numerical Results of the Quantum Mapping

For the quantum model discussed above, we have numerically iterate Eq. (16) by using Eqs. (21) and (23) to obtain the time evolution $\{b_n(N)\}$ starting from various initial $\{b_n(N)\}$ sets. Then we calculate at each iteration the average energy

$$\langle E\rangle = \left\langle \frac{1}{2}\hat{p}^2 + \frac{1}{2}\omega_0^2\hat{x}^2 \right\rangle = \sum_{n=0}^{\infty} E_n |b_n(N)|^2, \tag{24}$$

where we choose $\hbar = 1$. In all runs after fixing k, $\omega_0 T$ and T, we choose only a few (~ 4) adjacent $b_n(0)$ to be nonzero. Typical results are discussed below.

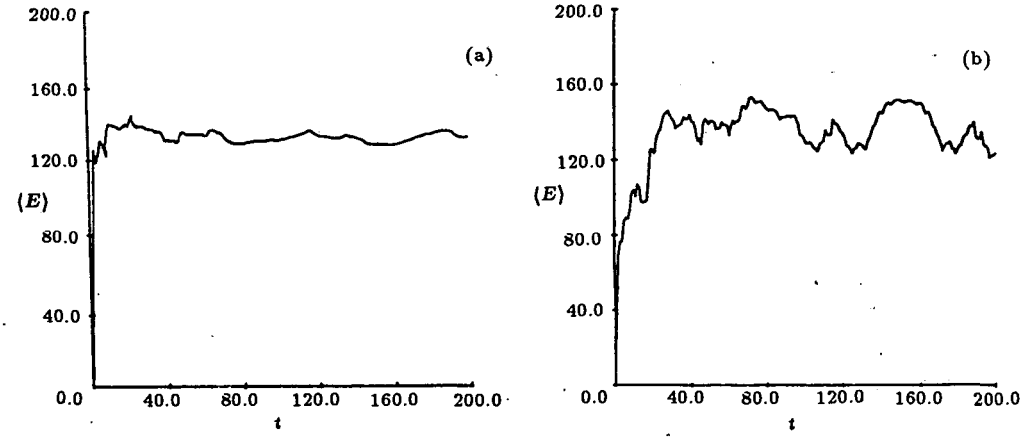

Fig. 1. Energy $\langle E\rangle$ of the quantum KHO mapping (16) for $\alpha = \omega_0 T = 2\pi(\sqrt{5}-1)/2$ and $T = 1$. (a) $k = 1.0$, (b) $k = 500$.

For $\omega_0 T = 2\pi(\sqrt{5}-1)/2$ and $T = 1$, we plot the numerically determined $\langle E\rangle$ versus time t in Fig. 1 at $k = 1.0\,(K = 0.77)$ and $k = 500\,(K = 386.5 \gg K_c = 4.2$ which is a critical value. When $K > K_c$, the classical motions of the KHO is completely chaotic). One can see from Fig. 1 tha' there is no distinct difference between Figs. 1a and 1b. At low or large k the energy increas' s very rapidly, roughly linear. However, this phenomenon persists only upto a time t_B, and then the energy growth saturates accompanied by fluctuations. The fluctuation

becomes larger for larger values of k. In Fig. 1a the saturate energy value is about 120.8 and the fluctuation $\langle (E - \langle E \rangle)^2 \rangle$ is about 0.4 which is about 2.2 in Fig. 1b. Empirically, we find that t_B is proportional to $1/\alpha$ and independent of k. A possible explanation of the appearance of this break-time t_B may line in the uncertainty relationship $\Delta E \Delta t \sim \hbar$. One notes from Eq. (8) that the classical limit $\hbar \to 0$ is equivalent to $k \to \infty$ (T and ω does not change) or $T \to 0$ (k does not change) for fixed K and α, that means whether k is large or small, we might expect the quantum behavior to mimic the classical at least for a time interval Δt during which the discrete nature of the free oscillator energy level spectrum is insignificant. If t_B is the time required for the quantum system to notice that energy levels are discrete, that is $\Delta t \sim t_B$. From Eq. (22), one notes that α is a measure of the effective energy level spacing. Thus taking $\Delta E \sim \alpha$ in $\Delta E \Delta t \sim \hbar$, we have $t_B \sim 1/\alpha$. The relationship shows that the quantum mapping is not affected by the value k.

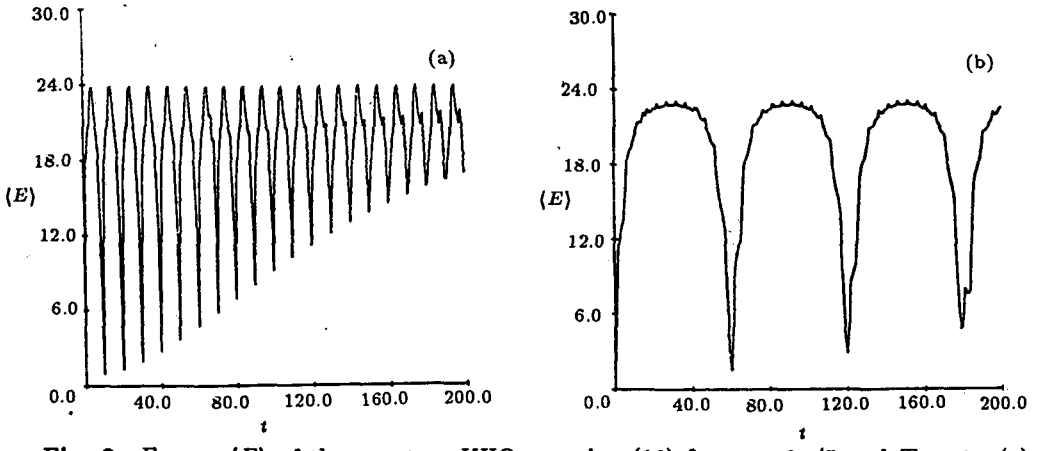

Fig. 2. Energy $\langle E \rangle$ of the quantum KHO mapping (16) for $\alpha = 2\pi/5$ and $T = 1$. (a) $k = 1.0$, (b) $k = 500$.

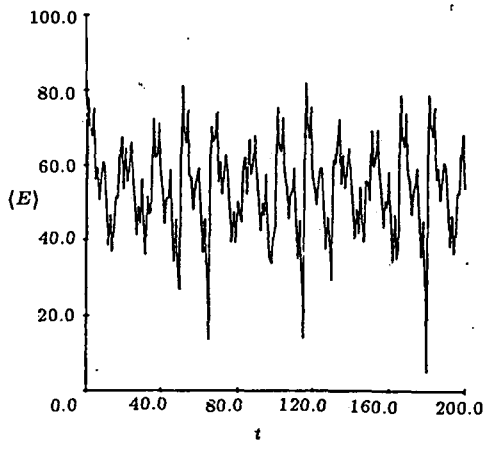

Fig. 3. Energy $\langle E \rangle$ of the quantum KHO mapping (16) for $\alpha = 2\pi/5$, $T = 4$ and $k = 500$.

For $\omega_0 T/2\pi = r/s$ (t and s are integers, $r < s$), the result of the quantum mapping is very different from the kicked rotator. In Fig. 2 we present two pictures for the behavior of the energy as a function of time with $\omega_0 T = 2\pi/5$, $T = 1$, and $k = 0.8$ ($K = 0.4$) and $k = 500$ ($K = 410 \gg K_c = 2.7$), respectively. One notices that the energy is damped oscillation (see Figs. 2a and 2b). For fixed α and k and increasing the kick period T, we obtain a picture of energy recurrence as shown in Fig. 3 (in Fig. 3 the values of α and k are the same as those in Fig. 2b). The difference between Fig. 2b and Fig. 3 might be caused by

the $C_{nm,l}$. From Eq. (21) one can note that for large T thus smaller ω_0 and larger $1/\omega_0$ (for fixed α) the value of $C_{nm,l}$ is more important for the same (n, m). Thus the zero off-diagonal matrix elements of w are larger so that the energy varying with time might be more random as shown in Fig. 3. Further numerical results for $\omega_0 T/2\pi = r/s$ indicate that there is no resonance case as in a kicked rotator, except for $\omega_0 T = 4n\pi$ discussed below.

III. Discussion and Conclusion

Our numerical study indicates that the behavior of the quantum KHO is different from that of the quantum kicked rotator (the latter depends on the strength of the kick force). Working with an irrational $\omega_0 T/2\pi$, we found numerically a saturation phenomenon that the break-time t_B is proportional to $1/\alpha$ and independent of k. When $\omega_0 T/2\pi$ is rational and the kick period T is low, the energy $\langle E\rangle$ is damped oscillation with time. For larger value of T, we have obtained a picture of energy recurrence in the sense of Hogg and Huberman[11].

Another feature of the KHO is the existence of resonance for $\omega_0 T$ equal to some multiple 4π. Just as done for the kicked quantum rotator in Ref. [1], over any period T between delta function kicks the $a(t)$ evolves according to

$$a_n(t+T) = a_n(t)e^{-i\varepsilon_n T} \tag{25}$$

over the infinitesimal interval $(t+T^-)$ to $(t+T^+)$

$$\phi(x, , t+T^+) = e^{ik\cos x}\phi(x, t+T^-)\,. \tag{26}$$

Regardless of k-value or initial $\phi(x, 0)$, the free oscillator mapping of Eq. (25) is the identity map when $\omega_0 T = j4\pi$ (j is an integer). For $\omega_0 T$-values after a number t of kicks, we have from Eq. (26) that $\phi(t) = \exp(itk\cos x)\phi(0)$ which yields the average energy growth given by

$$\langle E\rangle = \int dx\phi^*\Big(-\frac{1}{2}\frac{\partial^2}{\partial x^2} + \frac{1}{2}\omega_0^2 x^2\Big)\phi \sim t^2 \tag{27}$$

that is proportional to t^2 for large t, corresponding to resonance. This result is also validated by the numerical method discussed above. In this sense, we can say that α in the quantum KHO model acts as τ in the kicked rotator[1], but the nature of the energy behavior in these two models is different. Specially, regardless of k, ω_0 and T, there is no stochastic energy diffusion in the KHO system considered herein.

References

[1] G. Casati, B.V. Chirikov, F.M. Izrailev and J. Ford, in Springer Lecture Notes in Physics, ed. by G. Casati and J. Ford, Springer, New York, Vol. 93, (1979).

[2] B.V. Chirikov, Phys. Rep. **52**(1979)263.

[3] F.M. Izrailev and D.L. Shepelyanskii, Sov. Phys. Dokl. **24**(1979)996; B. Dorizzi *et al.*, J. Stat. Phys. **37**(1984)93.

[4] D.R. Grempel, S. Fishman and R.E. Prang, Phys. Rev. Lett. **49**(1982)833; D.R. Grempel *et al.*, Phys. Rev. **A29**(1984)1639.

[5] For an up-to-date review of quantum chaos, see R.V. Jensen, Nature **355**(1992)311.

[6] A.A. Chernikov, R.Z. Sagdeev, D.A. Usikov, M.Yu Zakharov and G.M. Zaslavsky, Nature **326**(1987)559.

[7] R.H.G. Helleman, "*Fundamental Problems in Statistical Mechanics (V)*", ed. by E.G.D. Cohen, North-Holland (1980).

[8] D. Shechtman, I. Blech, D. Gratias and J.W. Chan, Phys. Rev. Lett. **53**(1984)1951.

[9] G.M. Zaslavsky, M.Yu Zakharov, R.Z. Sagdeev, D.A. Usikov and A.A. Chernikov, Zh. Eksp. Teor. Fiz. **89**(1986)500.

[10] A.J. Lichtenberg and B.P. Wood, Phys. Rev. Lett. **62**(1989)2213; Phys. Rev. **A39**(1989)2153.

[11] T. Hogg and B.A. Huberman, Phys. Rev. Lett. **48**(1982)711.